



MRI of gallbladder cancer

Cher Heng Tan, Kian Soon Lim

ABSTRACT

Gallbladder cancer, the most common of biliary tract cancer, is often diagnosed at an advanced stage with ensuing poor survival rates. Imaging may allow for earlier diagnosis, however there may be significant overlap with nonmalignant conditions of the gallbladder in early stages of cancer. In this pictorial essay, we use various examples to describe the utility of magnetic resonance imaging in the diagnosis and staging of gallbladder cancer, noting in particular the strengths and limitations of the imaging modality. The use of diffusion-weighted imaging as an adjunct technique for diagnosis is also discussed.

Gallbladder cancer (GBCA) is considered relatively rare, accounting for only 1%–2% of all alimentary tract malignancies (1). The Surveillance, Epidemiology, and End Results (SEER) Program recorded 5723 GBCA cases between 1988–2001 in the USA (2). Nevertheless, GBCA remains the most common biliary tract cancer, with a higher prevalence than other extrahepatic biliary cancers, such as those arising from the ampulla of Vater. At histological analysis, approximately 90% of GBCAs are adenocarcinomas (3). GBCA has striking genetic, racial, and geographic characteristics (4, 5). It is three times more common in women than men, and typically occurs in patients 65 years and older (6).

Clinical presentation and risk factors

Affected patients usually present with nonspecific symptoms of jaundice and indigestion that can be identical to symptoms of benign gallbladder disease, such as choledocholithiasis (7). The main risk factors for GBCA include cholelithiasis (especially untreated chronic symptomatic gallstones), obesity, and chronic gallbladder infections (5, 8). Less common associations include anomalous junction of pancreaticobiliary ducts and porcelain gallbladder (up to 20% of patients) (5). Some authors recommend prophylactic cholecystectomy in high-risk groups (5, 8).

Role of imaging

Early GBCA frequently presents as incidental gallbladder lesion during radiological workup for abdominal complaints, with nonspecific imaging appearances. Significant overlap between GBCA and benign diseases of the gallbladder often exist on imaging, and even on histopathology (9).

Radiologist awareness and familiarity with these findings can lead to early diagnosis and a curative outcome. Accurate assessment of the extent of the disease is vital in treatment planning and prognostication. Although ultrasonography and computed tomography (CT) are most commonly used in investigating gallbladder pathologies, increasing evidence has supported the superiority of magnetic resonance imaging (MRI). MRI offers superior soft tissue delineation of gallbladder lesions and biliary tree. Functional techniques, such as diffusion-weighted imaging (DWI), provides useful information on the malignant potential of nonspecific lesions and detection of metastases.

MRI

MRI sequences should be tailored to the clinical question. T2-weighted sequences (usually fast spin-echo sequences with respiratory gating) are optimal for evaluating soft tissue abnormalities involving the wall of the gallbladder. The section thickness should be 5 mm or less, with a 1–2 mm

From the Department of Diagnostic Radiology (C.H.T. ✉ tchers1977@gmail.com), Tan Tock Seng Hospital, Singapore, Singapore

Received 20 November 2012; revision requested 16 December 2012; revision received 24 January 2013; accepted 26 January 2013

Published online 17.04.2013
DOI 10.5152/dir.2013.044

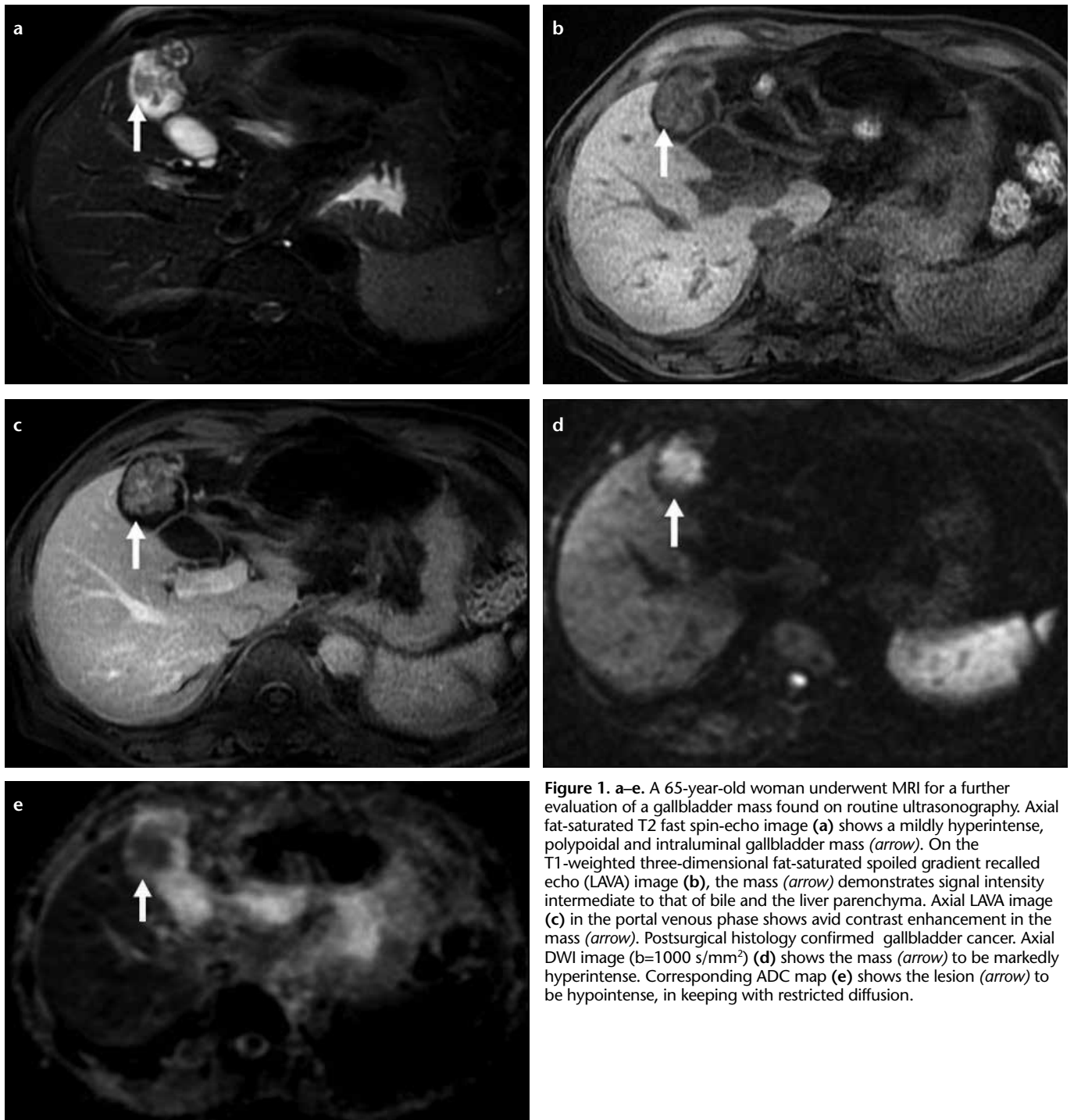


Figure 1. a–e. A 65-year-old woman underwent MRI for a further evaluation of a gallbladder mass found on routine ultrasonography. Axial fat-saturated T2 fast spin-echo image (a) shows a mildly hyperintense, polypoidal and intraluminal gallbladder mass (arrow). On the T1-weighted three-dimensional fat-saturated spoiled gradient recalled echo (LAVA) image (b), the mass (arrow) demonstrates signal intensity intermediate to that of bile and the liver parenchyma. Axial LAVA image (c) in the portal venous phase shows avid contrast enhancement in the mass (arrow). Postsurgical histology confirmed gallbladder cancer. Axial DWI image ($b=1000 \text{ s/mm}^2$) (d) shows the mass (arrow) to be markedly hyperintense. Corresponding ADC map (e) shows the lesion (arrow) to be hypointense, in keeping with restricted diffusion.

gap between sections. Useful additional T2-weighted sequences are similar to those used to evaluate the biliary tree (magnetic resonance cholangiopancreatography [MRCP]) (Figs. 1 and 2): heavily T2-weighted fluid sensitive acquisition techniques such as half-fourier acquisition single-shot turbo spin echo (HASTE).

Although T1-weighted MRI of the gallbladder can be performed with

spin-echo or breath-hold spoiled gradient-echo techniques, the latter are superior because they decrease respiratory artifacts. Dynamic contrast material-enhanced fat-suppressed T1-weighted MRI sequences improve the delineation of the gallbladder wall and bile ducts, and allow assessment of the liver parenchyma for tumor invasion and metastatic disease (10). In addition, we routinely

perform DWI using respiratory-triggered (navigator-echo technique) fat-suppressed single-shot echo planar imaging in the axial plane. Tri-directional diffusion gradients using three b values (0, 500, 1000 s/mm^2) are applied within a single acquisition. Parallel imaging with an acceleration factor of two is applied to shorten scan duration. Trace diffusion images are displayed for each

b value acquired. Pixel-based apparent diffusion coefficient (ADC) maps are routinely generated to reduce false positives related to T2 shine through.

MRI features

In a series of 19 patients undergoing MRI, the predominant patterns of GBCA were of mass-forming and diffuse wall thickening (Figs. 1 and 2) (11). Schwartz et al. (12) showed that GBCA manifested at MRI as focal gallbladder wall thickening with an eccentric mass in 76% of cases. GBCA is typically T1 hypointense and T2 hyperintense compared with the surrounding liver parenchyma (Figs. 2 and 3). Concurrent presence of gallstones is common, and better demonstrated on MRI than on CT. GBCAs show enhancement after administration of gadolinium-based contrast material. Irrespective of configuration, GBCA typically shows early irregular contrast enhancement, which persists into delayed images. The sensitivity and specificity of MRI for a gallbladder lesion of 0.8 cm size and for the presence of gallbladder neoplasia was 100% (95% confidence interval [CI], 77%–100%) and 70% (95% CI, 35%–93%), respectively (13).

Differential diagnoses

Perhaps the most challenging task for radiologists in imaging GBCA is its identification amongst many radiologically similar benign gallbladder pathologies. A variety of benign gallbladder pathologies may manifest as gallbladder polypoid lesions or wall thickening. Differentiation between these lesions and early GBCA requires prudence, appropriate imaging techniques, and familiarity with subtle differentiating features. Here, MRI holds its utmost superiority over other modalities.

Acute cholecystitis

Suggestive clinical findings, a distended gallbladder in the presence of a cystic duct or a gallbladder neck calculus, and the presence of pericholecystic fluid are important, but not omnipresent findings of acute cholecystitis (14, 15). On HASTE images, the wall thickening in acute cholecystitis is typified by an ill-defined double-layered pattern; a broadened or interrupt-

ed hypointense inner layer (composed of mucosa and muscle) is surrounded by a thick hyperintense outer layer (composed of edematous stroma and serosa) (Fig. 3) (16). Gangrenous cholecystitis is complicated of ischemic necrosis of the gallbladder wall with the double-layered pattern replaced by a single irregular layer on imaging, mimicking GBCA (16). Clinical correlation and presence of ancillary findings (e.g., pericholecystic free fluid) are vital. Rarely, GBCA and acute cholecystitis coexist due to their common association with calculous disease.

Chronic cholecystitis

The nonspecific and insidious clinical presentation of chronic cholecystitis makes its clinical differentiation from GBCA impossible. As with the acute form, chronic cholecystitis manifests as well-defined, double-layered wall thickening on imaging, with a thin hypointense inner layer and a thick hyperintense outer layer on HASTE images (16). Enhancement of the inner layer in chronic cholecystitis is usually smooth and early, followed by delayed enhancement of the outer layer (Fig. 4). Enhancement in GBCA is usually irregular, occurs early and remains prolonged (17, 18). Hence, high resolution T2 and arterial phased contrast enhanced images are most useful in differentiating GBCA from inflammatory wall thickening. The late phases of enhancement are less useful, as delayed wall enhancement is present in both cholecystitis and GBCA (12).

Xanthogranulomatous cholecystitis, an uncommon form of chronic cholecystitis, is notorious for mimicking GBCA, both clinically and on imaging (Fig. 5). Its typical imaging features are mass-like wall thickening, local invasion and regional adenopathy. MRI findings of xanthogranulomatous cholecystitis include areas of iso- to mild hyperintensity on T2-weighted images, which show slight enhancement at early phase and strong enhancement at late phase on dynamic study, corresponding with areas of abundant xanthogranulomas. Areas with very high signal intensity on T2-weighted images without enhancement correspond to necrosis or abscess (Fig. 5). Notwithstanding, preoperative differentiation

between xanthogranulomatous cholecystitis and GBCA on imaging remains challenging.

Gallbladder adenomyomatosis

The “pearl necklace” on heavily T2 images, which indicates the presence of Rokitansky-Aschoff sinuses within the thickened gallbladder wall, was reported to carry high accuracy for gallbladder adenomyomatosis (19). However, the true specificity of this sign has not been tested against GBCA. Hence, presence of regional intramural cystic spaces still warrants regular imaging follow-up.

Benign polyps

Small polyps are common incidental gallbladder lesions and larger ones can mimic polypoid GBCA. Small size (<1 cm), multiplicity, and stalked configuration favor benignity. Large size (>10 mm), rapid growth, sessile or wide-based configuration, long pedicles, patient age over 50, concurrent gallstones, and infundibular location favor malignancy (20, 21). Malignant polypoid lesions typically demonstrate early and prolonged enhancement. In contrast, benign lesions demonstrate early enhancement with subsequent washout (22).

Added value of functional MRI

DWI uses the ability of water molecules to diffuse freely in biological tissue. DWI has been studied extensively for its capability in differentiating malignant from benign diseases in various abdominal organs, including the gall bladder. In theory, GBCA, with its high cellularity, will exhibit significant diffusion restriction and appear hyperintense on high b value DWI and yield low ADC value.

Using the same imaging criteria, Sugita et al. (23) reported that DWI carried an ADC value of over 0.94, with mean sensitivity and specificity rates of 83.3% and 100%, respectively, for differentiating GBCA from benign entities (including chronic cholecystitis, adenomyomatosis, and polyps) by DWI ($b=1000 \text{ s/mm}^2$). In a study of 10 benign (three hyperplastic polyps and seven adenomas) and 13 malignant (all adenocarcinomas) polypoid gallbladder lesions, Irie et al. (24) reported

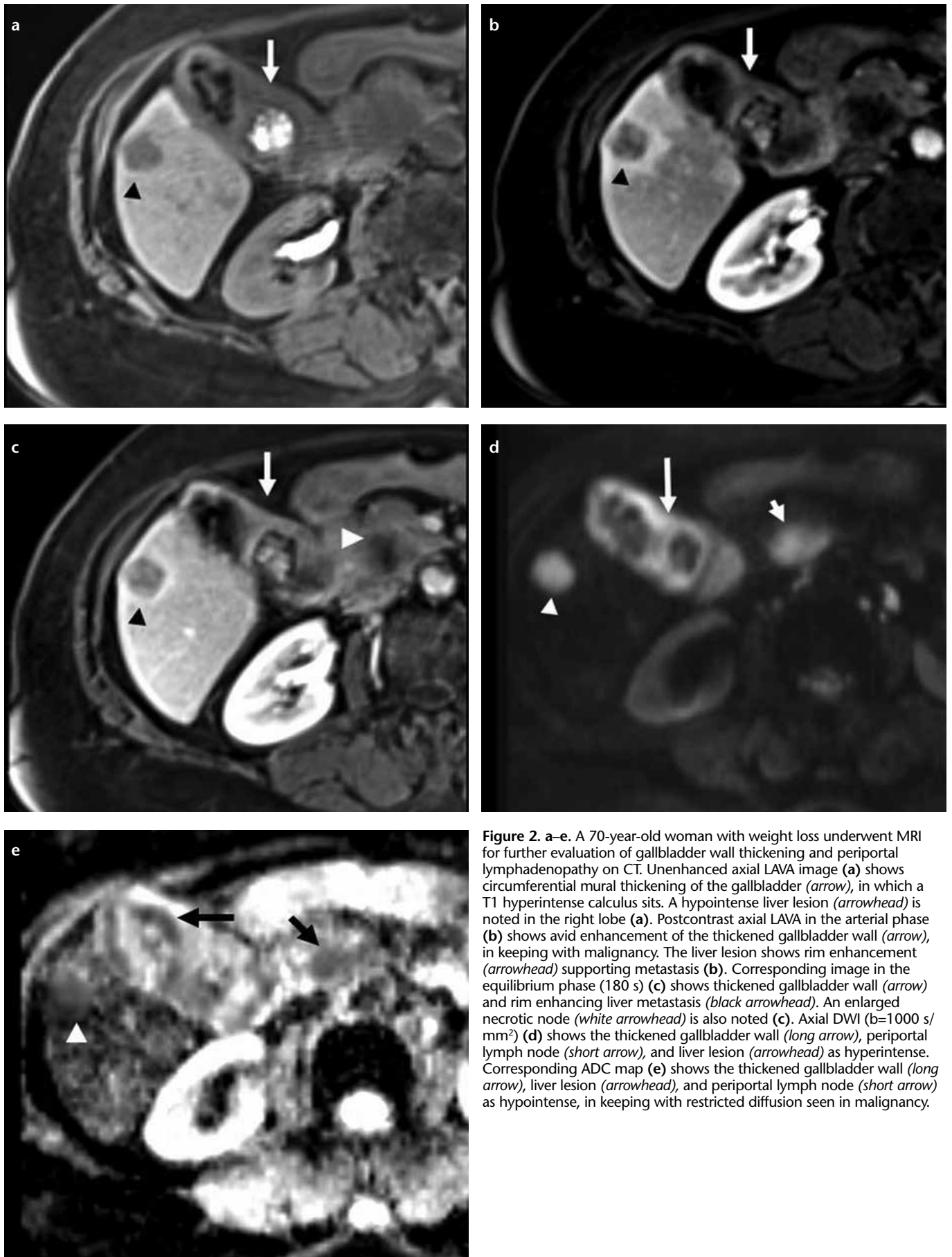


Figure 2. a–e. A 70-year-old woman with weight loss underwent MRI for further evaluation of gallbladder wall thickening and periportal lymphadenopathy on CT. Unenhanced axial LAVA image (a) shows circumferential mural thickening of the gallbladder (arrow), in which a T1 hyperintense calculus sits. A hypointense liver lesion (arrowhead) is noted in the right lobe (a). Postcontrast axial LAVA in the arterial phase (b) shows avid enhancement of the thickened gallbladder wall (arrow), in keeping with malignancy. The liver lesion shows rim enhancement (arrowhead) supporting metastasis (b). Corresponding image in the equilibrium phase (180 s) (c) shows thickened gallbladder wall (arrow) and rim enhancing liver metastasis (black arrowhead). An enlarged necrotic node (white arrowhead) is also noted (c). Axial DWI ($b=1000 \text{ s/mm}^2$) (d) shows the thickened gallbladder wall (long arrow), periportal lymph node (short arrow), and liver lesion (arrowhead) as hyperintense. Corresponding ADC map (e) shows the thickened gallbladder wall (long arrow), liver lesion (arrowhead), and periportal lymph node (short arrow) as hypointense, in keeping with restricted diffusion seen in malignancy.

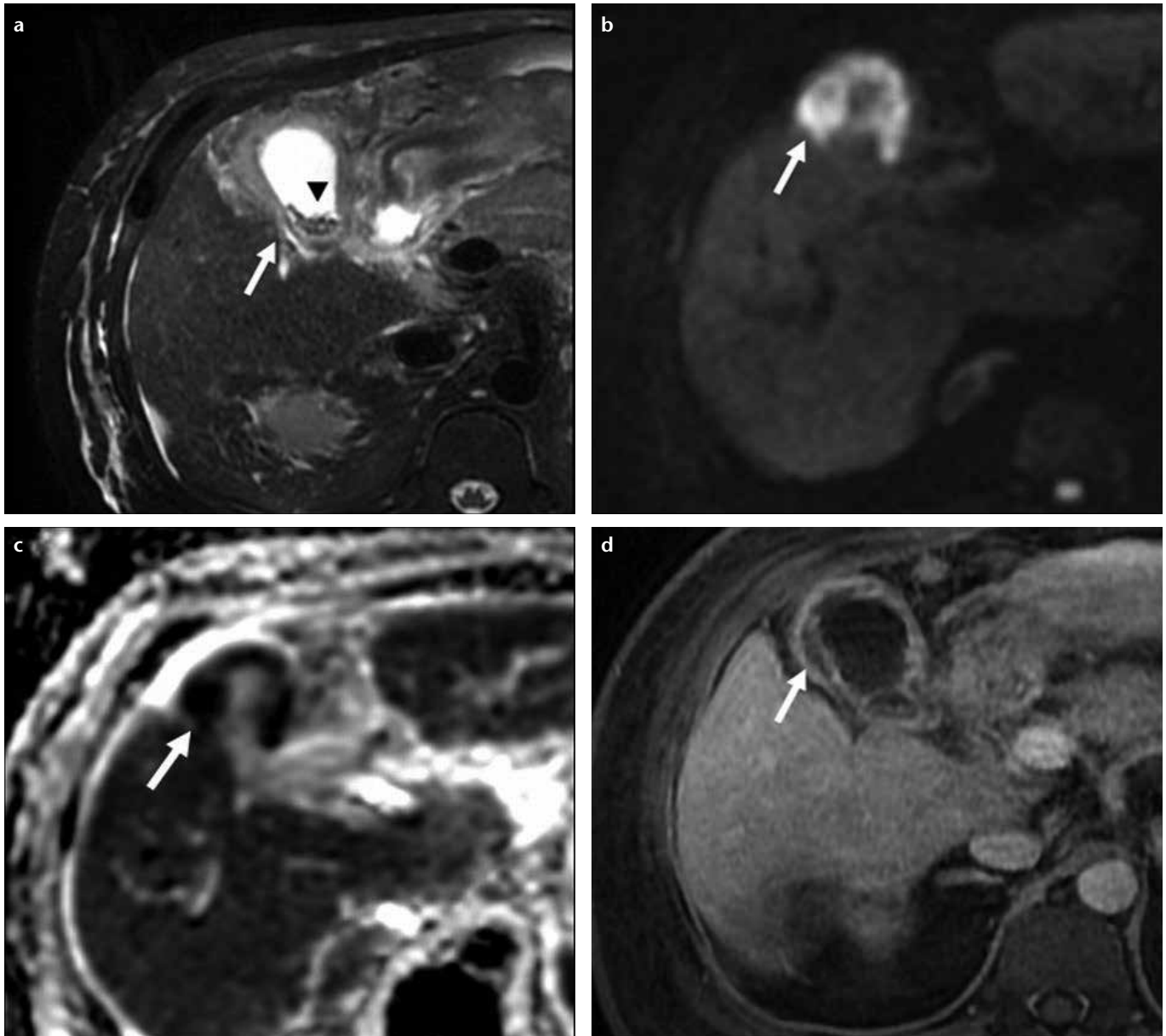


Figure 3. a–d. A 62-year-old man presenting with right upper quadrant pain. Axial fat-saturated T2 fast spin-echo image (**a**) shows double-layered wall thickening (*arrow*) of the gallbladder with intermediate intensity and trace pericholecystic fluid. Multiple small stones are present (**a**, *arrowhead*). DWI ($b=1000 \text{ s/mm}^2$) (**b**) shows fundal wall thickening as mass-like hyperintense lesion (*arrow*). Corresponding ADC map image (**c**) confirms restricted diffusion in the thickened fundal wall (*arrow*), a finding worrisome for malignancy. Axial contrast-enhanced LAVA image (**d**) in the equilibrium phase shows double-layered wall thickening (*arrow*) with smooth enhancement of the thin inner layer (mucosa), in keeping with acute cholecystitis. The diagnosis was confirmed on histology.

that 12 malignant lesions appeared of high or very high signal on high b value DWI, while only four benign lesions appeared of high signal on DWI. Both studies reported lower ADC values with GBCA than benign lesions.

In our experience, GBCA consistently appears hyperintense on DWI (Figs. 1 and 2), with corresponding low signal on ADC maps. However, a significant proportion of inflammatory wall thickening may also exhibit similar findings (Figs. 3 and 4). Hence, DWI

findings have to be interpreted in the light of other findings on the morphological sequences (25).

Patterns of spread

Early spread of GBCA can be attributed to the absence of a submucosal layer in the gallbladder wall. Local spread occurs readily along the hepatoduodenal ligament and para-aortic region by direct invasion, nodal, vascular, and perineural modes. Direct liver invasion and portal tract invasion are the main

modes of hepatic spread from resectable GBCA (26).

Kondo et al. (27) classified the modes of tumor spread in GBCA into six distinct patterns: (1) hepatic hilum type (tumor in the neck infiltrating the hepatic hilum); (2) hepatic bed type (tumor penetrates the liver with or without contiguous spread to the gastrointestinal tract); (3) bed and hilum type (huge mass involving both the gallbladder bed and the hepatic hilum); (4) lymph node type (enlarged

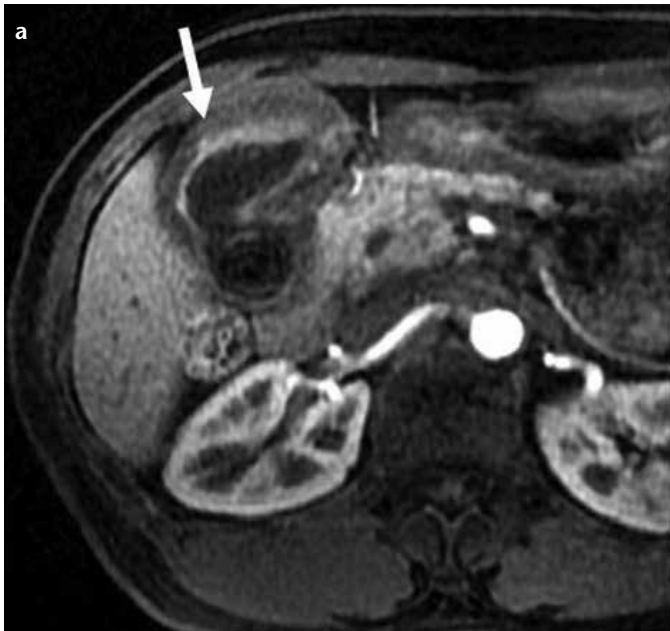


Figure 4. a, b. A 70-year-old man with a malignant cervical node of unknown origin underwent MRI for further evaluation of gallbladder wall thickening seen on CT. Axial postcontrast LAVA image in the arterial phase (**a**) shows diffuse double-layered thickening with no significant enhancement of the inner layer (*arrow*). Axial postcontrast LAVA equilibrium phase image (**b**) shows avid enhancement of the inner layer relative to the outer layer, and mild segmental enhancement of the outer layer (*arrow*). Image-guided needle biopsy showed chronic inflammation with fibrosis. No malignancy was seen.

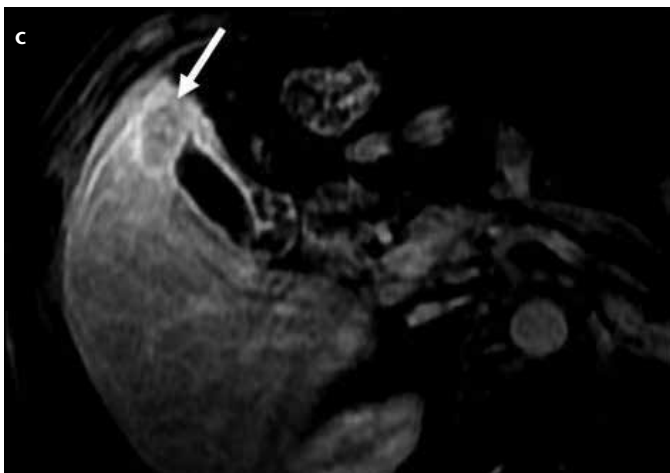
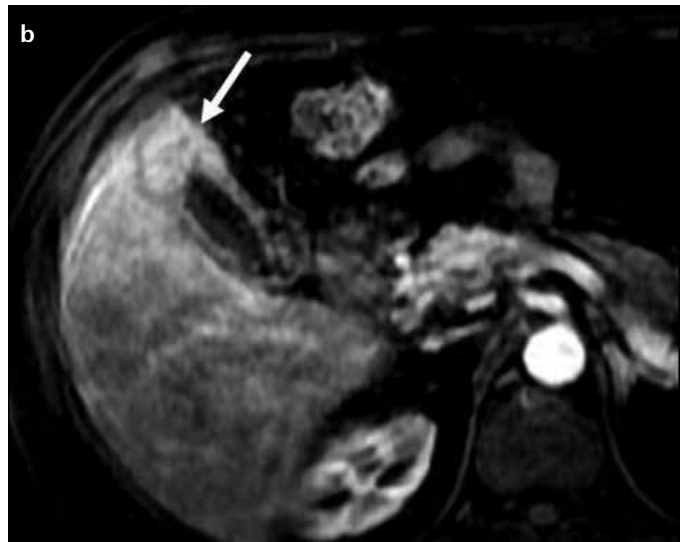
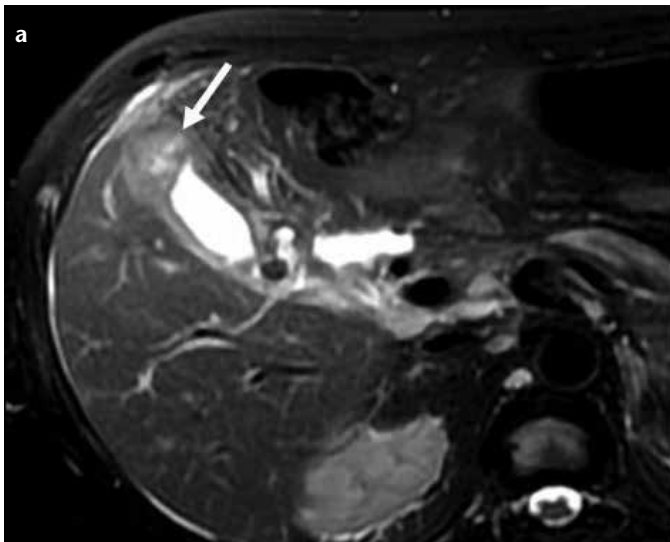


Figure 5. a-c. A 65-year-old woman with fever and right upper quadrant pain was found to have nonspecific gallbladder wall thickening on ultrasonography. Axial fat-saturated T2 fast spin-echo image (**a**) shows diffuse gallbladder wall thickening, most marked at the fundal region with intramural cystic foci (*arrow*). Corresponding axial contrast enhanced LAVA (portal venous phase) image (**b**) shows avid enhancement in the mass-like fundal thickening (*arrow*). Corresponding axial contrast enhanced LAVA (delayed phase) image (**c**) shows contrast washout in the thickened fundus (*arrow*), suggestive of an inflammatory process. Postcholecystectomy histology showed xanthogranulomatous cholecystitis.

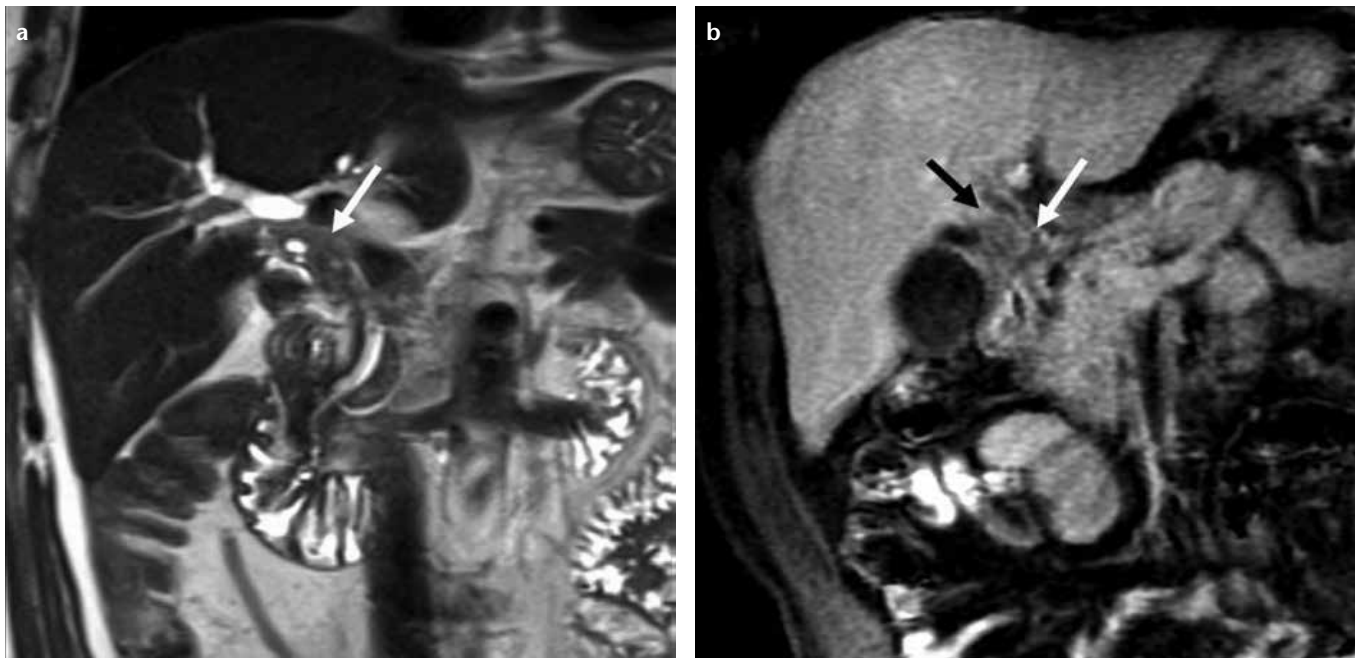


Figure 6. a, b. A 63-year-old man presenting with painless jaundice and found to have intrahepatic biliary dilatation on ultrasonography. Coronal single-shot fast spin echo image (a) confirms intrahepatic biliary dilatation, due to soft tissue infiltration mainly along the lateral aspect of the common hepatic duct (arrow). Coronal contrast enhanced LAVA image (b) shows the infiltrative mass (black arrow) to have arisen from the gallbladder neck, invading the cystic and common hepatic ducts (white arrow).

metastatic lymph nodes while the primary tumor remains limited to the gallbladder) (Fig. 2); (5) cystic duct type (small mass arising from the cystic duct) (Fig. 6); and (6) localized type tumor localized to the gallbladder) (27). Note that involvement of intercaecal nodes is classified as M1 disease (28).

Using an “all-in-one” MRI protocol, including MRCP and magnetic resonance angiography, the sensitivity and specificity of MRI examination were 100% and 89% for bile duct invasion, 100% and 87% for vascular invasion, 67% and 89% for hepatic invasion, and 56% and 89% for lymph node metastasis, respectively (29). Kaza et al. (30) showed that the sensitivity and specificity of using multiphasic MRI with MRCP in detecting hepatic invasion, lymph node metastasis and bile duct invasion was 87.5% and 86%, 60% and 90%, and 80% and 100%, respectively. Gadolinium-enhanced fat-suppressed T1-weighted images are most useful in diagnosing tumor extent, direct invasion of surrounding organs, liver metastases, and involvement of critical vascular structures such as the portal vein and hepatic artery (10). Overdiagnosis of duodenal invasion is usually related to the loss of fat plane due

to respiratory motion artifacts, partial volume effects and paucity of fat.

The additional value of DWI in assessing disease extent in GBCA has not been extensively studied. However, DWI has been shown to be highly accurate in detecting liver metastases from various primary malignancies (31–33). DWI is also highly sensitive in nodal detection although poorly specific in diagnosing malignant nodes. In our experience, DWI is particularly useful in detecting nodes around the liver hilum that can be elusive on morphological sequences.

Conclusion

GBCA is a lethal cancer typically diagnosed incidentally for routine cholecystectomy or by imaging. Widespread use of MRI for abdominal conditions makes it necessary for radiologists to be familiar with the strengths and limitations of this modality for GBCA diagnosis. We have also reviewed the pertinent MRI features of this condition that are useful in clinical practice.

Conflict of interest disclosure

The authors declared no conflicts of interest.

References

1. Franquet T, Montes M, Ruiz de Azua Y, Jimenez FJ, Cozcolluela R. Primary gallbladder carcinoma: imaging findings in 50 patients with pathologic correlation. *Gastrointest Radiol* 1991; 16:143–148. [CrossRef]
2. Howlader N, Noone AM, Krapcho M, et al. SEER Cancer Statistics Review, 1975–2008, National Cancer Institute. Available on http://seer.cancer.gov/csr/1975_2008/
3. Sohn TA, Lillemoe KD. Tumors of the gallbladder, bile ducts, and ampulla. In: Fedelman M, Friedman LS, Sleisenger MH, eds. *Sleisenger & Fortran's gastrointestinal and liver disease: pathophysiology/diagnosis/management*. 7th ed. Philadelphia: Saunders, 2003; 1153–1164.
4. Eslick GD. Epidemiology of gallbladder cancer. *Gastroenterol Clin North Am* 2010; 39:307–330. [CrossRef]
5. Sheth S, Bedford A, Chopra S. Primary gallbladder cancer: recognition of risk factors and the role of prophylactic cholecystectomy. *Am J Gastroenterol* 2000; 95:1402–1410. [CrossRef]
6. Levin B. Gallbladder carcinoma. *Ann Oncol* 1999; 10:129–130. [CrossRef]
7. Zatonski WA, Lowenfels AB, Boyle P, et al. Epidemiologic aspects of gallbladder cancer: a case-control study of the SEARCH Program of the International Agency for Research on Cancer. *J Natl Cancer Inst* 1997; 89:1132–1138. [CrossRef]
8. Lazcano-Ponce EC, Miquel JF, Munoz N, et al. Epidemiology and molecular pathology of gallbladder cancer. *CA Cancer J Clin* 2001; 51:349–364. [CrossRef]

9. Giang TH, Ngoc TT, Hassell LA. Carcinoma involving the gallbladder: a retrospective review of 23 cases-pitfalls in diagnosis of gallbladder carcinoma. *Diagn Pathol* 2012; 7:10. [\[CrossRef\]](#)
10. Catalano OA, Sahani DV, Kalva SP, et al. MR imaging of the gallbladder: a pictorial essay. *Radiographics* 2008; 28:135–155. [\[CrossRef\]](#)
11. Sagoh T, Itoh K, Togashi K, et al. Gallbladder carcinoma: evaluation with MR imaging. *Radiology* 1990; 174:131–136.
12. Schwartz LH, Black J, Fong Y, et al. Gallbladder carcinoma: findings at MR imaging with MR cholangiopancreatography. *J Comput Assist Tomogr* 2002; 26:405–410. [\[CrossRef\]](#)
13. Eaton JE, Thackeray EW, Lindor KD. Likelihood of malignancy in gallbladder polyps and outcomes following cholecystectomy in primary sclerosing cholangitis. *Am J Gastroenterol* 2012; 107:431–439. [\[CrossRef\]](#)
14. Park MS, Yu JS, Kim YH, et al. Acute cholecystitis: comparison of MR cholangiography and US. *Radiology* 1998; 209:781–785.
15. Regan F, Schaefer DC, Smith DP, Petronis JD, Bohlman ME, Magnuson TH. The diagnostic utility of HASTE MRI in the evaluation of acute cholecystitis. Half-Fourier acquisition single-shot turbo SE. *J Comput Assist Tomogr* 1998; 22:638–642. [\[CrossRef\]](#)
16. Jung SE, Lee JM, Lee K, et al. Gallbladder wall thickening: MR imaging and pathologic correlation with emphasis on layered pattern. *Eur Radiol* 2005; 15:694–701. [\[CrossRef\]](#)
17. Demachi H, Matsui O, Hoshiba K, et al. Dynamic MRI using a surface coil in chronic cholecystitis and gallbladder carcinoma: radiologic and histopathologic correlation. *J Comput Assist Tomogr* 1997; 21:643–651. [\[CrossRef\]](#)
18. Yoshimitsu K, Honda H, Kaneko K, et al. Dynamic MRI of the gallbladder lesions: differentiation of benign from malignant. *J Magn Reson Imaging* 1997; 7:696–701. [\[CrossRef\]](#)
19. Haradome H, Ichikawa T, Sou H, et al. The pearl necklace sign: an imaging sign of adenomyomatosis of the gallbladder at MR cholangiopancreatography. *Radiology* 2003; 227:80–88. [\[CrossRef\]](#)
20. Matos AS, Baptista HN, Pinheiro C, Martinho F. Gallbladder polyps: how should they be treated and when? *Rev Assoc Med Bras* 2010; 56:318–321. [\[CrossRef\]](#)
21. Yang HL, Sun YG, Wang Z. Polypoid lesions of the gallbladder: diagnosis and indications for surgery. *Br J Surg* 1992; 79:227–229. [\[CrossRef\]](#)
22. Tseng JH, Wan YL, Hung CF, et al. Diagnosis and staging of gallbladder carcinoma. Evaluation with dynamic MR imaging. *Clin Imaging* 2002; 26:177–182. [\[CrossRef\]](#)
23. Sugita R, Yamazaki T, Furuta A, Itoh K, Fujita N, Takahashi S. High b value diffusion-weighted MRI for detecting gallbladder carcinoma: preliminary study and results. *Eur Radiol* 2009; 19:1794–1798. [\[CrossRef\]](#)
24. Irie H, Kamochi N, Nojiri J, Egashira Y, Sasaguri K, Kudo S. High b value diffusion-weighted MRI in differentiation between benign and malignant polypoid gallbladder lesions. *Acta Radiol* 2011; 52:236–240. [\[CrossRef\]](#)
25. Smith AD, Veniero JC. Gd-EOB-DTPA as a functional MR cholangiography contrast agent: imaging gallbladder filling in patients with and without hepatobiliary dysfunction. *J Comput Assist Tomogr* 2011; 35:439–445. [\[CrossRef\]](#)
26. Wakai T, Shirai Y, Sakata J, Nagahashi M, Ajioka Y, Hatakeyama K. Mode of hepatic spread from gallbladder carcinoma: an immunohistochemical analysis of 42 hepatectomized specimens. *Am J Surg Pathol* 2010; 34:65–74. [\[CrossRef\]](#)
27. Kondo S, Nimura Y, Kamiya J, et al. Mode of tumor spread and surgical strategy in gallbladder carcinoma. *Langenbecks Arch Surg* 2002; 387:222–228. [\[CrossRef\]](#)
28. Bartlett DL. Gallbladder cancer. *Semin Surg Oncol* 2000; 19:145–155. [\[CrossRef\]](#)
29. Kim JH, Kim TK, Eun HW, et al. Preoperative evaluation of gallbladder carcinoma: efficacy of combined use of MR imaging, MR cholangiography, and contrast-enhanced dual-phase three-dimensional MR angiography. *J Magn Reson Imaging* 2002; 16:676–684. [\[CrossRef\]](#)
30. Kaza RK, Gulati M, Wig JD, Chawla YK. Evaluation of gall bladder carcinoma with dynamic magnetic resonance imaging and magnetic resonance cholangiopancreatography. *Australas Radiol* 2006; 50:212–217. [\[CrossRef\]](#)
31. Nasu K, Kuroki Y, Nawano S, et al. Hepatic metastases: diffusion-weighted sensitivity-encoding versus SPIO-enhanced MR imaging. *Radiology* 2006; 239:122–130. [\[CrossRef\]](#)
32. Koh DM, Brown G, Riddell AM, et al. Detection of colorectal hepatic metastases using MnDPDP MR imaging and diffusion-weighted imaging (DWI) alone and in combination. *Eur Radiol* 2008; 18:903–910. [\[CrossRef\]](#)
33. Bruegel M, Gaa J, Waldt S, et al. Diagnosis of hepatic metastasis: comparison of respiration-triggered diffusion-weighted echo-planar MRI and five t2-weighted turbo spin-echo sequences. *AJR Am J Roentgenol* 2008; 191:1421–1429. [\[CrossRef\]](#)